

Computational evaluation of N-16 measurements for a 14 MeV neutron irradiation of an ITER first wall component with water circuit



C.R. Nobs^{a,*}, J. Naish^a, L.W. Packer^a, R. Worrall^a, M. Angelone^b, A. Colangeli^b, S. Loreti^b, M. Pillon^b, R. Villari^b

^a Culham Centre for Fusion Energy, Culham Science Centre, Abingdon, Oxon, OX14 3DB, UK

^b ENEA - Department of Fusion and Technology for Nuclear Safety and Security via E. Fermi 45, 00044 Frascati (Rome), Italy

ARTICLE INFO

Keywords:

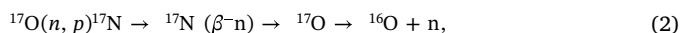
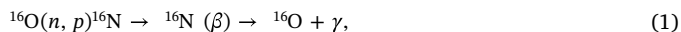
Neutronics
Neutron detector
FNG
neutron activation

ABSTRACT

During ITER operations the water coolant flowing through components such as the first wall, blanket modules, divertor cassettes and vacuum vessel will become activated by high energy neutrons. Two key neutron-induced reactions will occur with oxygen in the water producing the radioactive isotopes N-16 and N-17, which have relatively short half-lives of a few seconds. These nuclides are transported in coolant loops and, unmitigated, their decay emissions will induce additional nuclear heat in components, potentially including superconducting magnets, and lead to an increase in the occupational dose for workers and sensitive equipment outside the biological shield. Variations in irradiation, water flow rate and cooling circuit parameters make it difficult to predict nuclear heating. A water activation experiment has recently been performed at the 14 MeV Frascati Neutron Generator to accurately measure N-16 and N-17 produced by irradiating an ITER first wall mock-up. This experiment aimed to validate the methodology for water activation assessment used for ITER and to provide scientific justification to reduce safety factors, which have a large impact on ITER component design and qualification. This paper provides a detailed description of neutronics calculations performed together with the GammaFlow code to model the temporal evolution of activated water, along with MCNP6.1 and FISPACT-II to calculate the detector response. The calculated reaction rates associated with nuclear data from ten libraries have been compared with measured data, although as many cross-sections originated from the same library effectively five nuclear data libraries have been compared.

1. Introduction

The water coolant in ITER components such as those inside the first wall, blanket modules, divertor cassettes and vacuum vessel will become activated by neutrons during D-T plasma operations. Two key neutron induced reactions will occur with oxygen producing the radioactive nitrogen isotopes N-16 and N-17 through the following reactions:



Reaction 1 produces gamma rays at 6.128 MeV (gamma emission probability per disintegration, $I=67.0\%$) and 7.115 MeV ($I=4.9\%$), whereas reaction 2 produces delayed neutrons at 0.387 MeV ($I=35.8\%$), 0.886 MeV ($I=0.5\%$), 1.163 MeV ($I=47.6\%$), 1.690 MeV ($I=7.0\%$) and gamma rays at 0.870 MeV ($I=3.3\%$) [1]. Because water

coolant is being transported to other locations, the decay emissions from these nuclides will induce nuclear responses in sensitive tokamak and plant components, e.g. nuclear heat in superconducting magnets, absorbed doses in polymer-based components like valves, or high dose rates in electronics. The uncertainty in the calculation of radiation maps due to activated water is evaluated to be very large, the main sources of uncertainty being due to modelling ($\sim 200\%$) and nuclear data, hence safety factors between 8.2 and 4.7 are applied [2,3]. The motivation for this experiment is to accurately measure the N-16 and N-17 in an ITER-like environment with the aim to validate the methodology for water activation assessment used for ITER and provide a scientific justification to reduce these safety factors.

2. Experimental Setup

The ITER first wall (FW) mock-up was placed at 5 cm and 2 cm from the Frascati Neutron Generator (FNG) 14 MeV neutron source target

* Corresponding author.

E-mail address: chantal.nobs@ukaea.uk (C.R. Nobs).

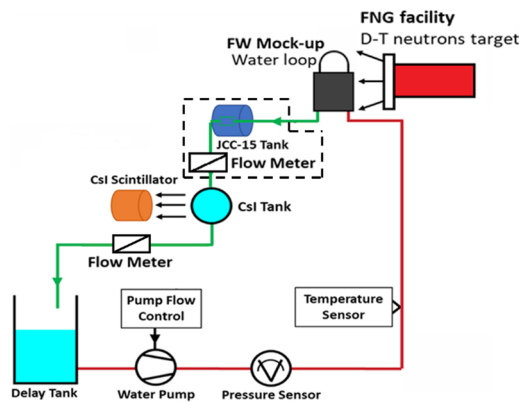


Fig. 1. Schematic drawing of the N-16 experimental flowing water circuit at the FNG, circuit #1 (excluding dashed box) consists of the mock-up connected to the CsI tank and the delay tank, whereas circuit #2 also includes the JCC-15 tank in the dashed box, and the flow meter was relocated between the JCC-15 tank and the CsI tank.

and connected to a water circuit illustrated in Figure 1.

A CsI detector was used to measure the gamma emission from N-16 and is described in Section 3.1, while a moderated He-3 detector (JCC-15) was used to measure the neutron emission from N-17 and is described in Reference [4]. Two versions of the water circuit were used during the FNG experiment. For circuit #1 the FW mock-up was connected directly to the CsI in-line water expansion tank (referred to as the CsI tank), whereas for circuit #2 the FW mock-up was connected to the in-line water expansion tank located inside the He-3 neutron detector ring (referred to as the JCC-15 tank and indicated in the dashed box in Figure 1), the JCC-15 tank was then connected to the CsI tank and the flow meter was relocated between the two tanks. Having two versions of the circuit provided more comprehensive experimental data to test the capabilities of the GammaFlow code [5], a tool developed in Python and make sure the system was modelled correctly. For circuit #1 17.4 m of plastic tubing (internal diameter 11 mm) connected the FW mock-up with the CsI tank with volume 0.1831 litres. 1.8 m of tubing (internal diameter 11 mm) connected the CsI tank with the 110 litre delay tank, and 18.4 m of tubing (internal diameter 28 mm) connected the delay tank with the FW mock-up with a volume experimentally determined as 0.322 litres. Whereas in circuit #2 17.4 m of plastic tubing (internal diameter 11 mm) connected the FW mock-up with the JCC-15 tank with volume 2.519 litres. 1.125 m of tubing (internal diameter 11 mm) connected the JCC-15 tank with the CsI tank, with the flow meter attached on this section of tubing. 0.5 m of tubing (internal diameter 11 mm) connected the CsI tank with the delay tank, and 20 m of tubing (internal diameter 25 mm) connected the delay tank with the FW mock-up. The reduced internal diameter of the tubing from the mock-up to the delay tanks (green line in Figure 1) reduced the transit time between irradiation and detection. The CsI expansion tank was made from aluminium, with a wall thickness of ~ 0.5 cm to support the water pressure, the purpose was to increase the total activity that is present in the detector region and hence the count rate by increasing the volume of activated water seen by the CsI detector, the volume of the expansion tanks was optimised prior to the experimental campaign. The purpose of the water delay tank was to ensure that an extensive number of N-16 nuclides had decayed before the water was pumped back to the mock-up, where the irradiation-measurement cycle restarts. The results for N-17 have not been considered in this paper, but are presented in Reference [4].

2.1. Experimental procedure

For circuit #1 the water pump frequency was set between 10-50 Hz, in steps of 5 Hz. Whereas for circuit #2 the water flow meter was

relocated to provide a more accurate reading for the benefit of the N-17 results presented in Reference [4] and the water pump frequency was set between 10-35 Hz, in steps of 5 Hz (for higher flow rates it was difficult to get an accurate reading as the flow meter had malfunctioned). The water flow was set in all cases without the presence of neutrons, a more detailed description of the experimental procedure can be found in Reference [6]. Taking measurements with the mock-up at both 5 cm and 2 cm from the FNG target optimised the results for both nuclides and provided a range of measurements to test the simulation methodologies. With the mock-up at 5 cm the net count rate after background subtraction was high for the CsI detector but very low for the JCC-15 detector, thus optimised for the detection of gamma-rays associated with N-16. Moving the mock-up to 2 cm increased the N-16 and N-17 production rate and subsequently the net count rate in the JCC-15 detector, thus optimised for the measurement of neutrons from N-17. Once the water flow rate had stabilised the deuteron beam was directed onto the FNG target to produce neutrons with a typical emission rate in the range of $1.3\text{--}2.0 \times 10^{10}$ neutrons/s for typical irradiation times of 150-300 seconds. The FNG emission rate is determined absolutely by counting the α particle associated with the neutrons produced in the D-T reaction [7]. The experimental results have been normalised to 1×10^{10} neutrons/s so that direct comparisons can be made between calculated results and experimental results and to make it easier to compare results at different flow rates and across the four measurement scenarios. The time-of-flight (TOF) between the FW mock-up and the CsI tank was derived from the profile of the count rate vs time, as illustrated in Figure 2. When activated water reaches the CsI tank there is a sharp rise in the count rate, and there is a change in gradient observed on this rise. For the example flow rate of 19.6 litres/min in Figure 2 the initial rise in count rate starts at 9.7 seconds which corresponds to the time required for partially activated water to travel from the outlet of the FW mock-up to the inlet of the CsI detector expansion tank (it takes 10.2 seconds to reach the outlet of the CsI expansion tank, as recorded in Table 1). The change in gradient at 10.3 seconds indicates the arrival of water from element #26 in the FW mock-up (which was divided into 64 mostly equal volume elements as illustrated in Figure 3) that had undergone longer irradiation, and the plateau at ≈ 10.6 seconds shows when water has travelled from element #64 in the FW mock-up having undergone the full irradiation and indicating the system has reached a steady state. The flow rate, calculated by dividing the sum of the volumes of the water from the FW mock-up by the TOF, was used to calculate the transit time through the FW mock-up using:

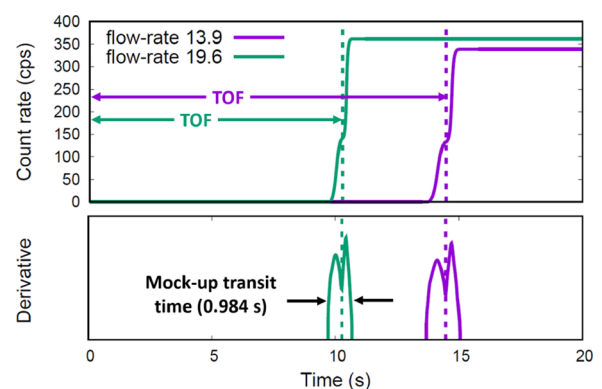


Fig. 2. A plot to indicate the methodology used to calculate the TOF reproduced using GammaFlow. The green and purple curves in the top plot show the activity build-up in the CsI tank for water flow rates 13.9 litres/min and 19.6 litres/min respectively for the ENDF/B-VII.0 nuclear data library, with the mock-up positioned at 2 cm. The bottom plot shows the first derivative of the top plot, and the central dip corresponds to the TOF for element #26 in the mock-up to reach the CsI tank.

$$\text{transit time} = \frac{0.322}{\text{water flow}}, \quad (3)$$

where 0.322 litres is the volume of the FW mock-up. For a flow rate of 19.6 litres/min Equation (3) calculates a transit time of 0.986 seconds showing good agreement with the transit time 0.984 seconds calculated using GammaFlow.

3. Neutron transport and activation calculations

To calculate the N-16 and N-17 reaction rates a well-characterised MCNP model of the FNG facility [7] was integrated with a model for the FW mock-up created from the technical drawings provided by ENEA, illustrated in Figure 3 where the FNG model is shown in green, the mock-up in blue and the water in purple. The CAD model was converted into MCNP geometry and run using MCNP6.1 [8]. The water is assumed to be free of impurities with a natural abundance of oxygen (99.757% O-16, 0.038% O-17 and 0.205% O-18 [1]), resulting in the atom fractions H-1 6.667×10^{-1} , O-16 3.325×10^{-1} , O-17 1.267×10^{-4} and O-18 6.833×10^{-4} [9]. FENDL-3.1d [10] cross-sections were used for all material definitions which included stainless steel for the tubes, Al-Si316LN for the body and CuCrZr for the section facing FNG target, detailed material data sheets were provided by F4E. During the experiment at ENEA aluminium struts were used to support the FW mock-up in-front of the FNG, the addition of a representative aluminium block behind the mock-up in the MCNP model resulted in a total percentage difference of N-16 atoms produced per source neutron per cm^3 across the full mock-up of $< 0.34\%$ and therefore detailed modelling of the aluminium struts was deemed unnecessary and not included in the final MCNP model.

The GammaFlow code [5] assumes the system consists of straight cylindrical pipes with sections of variable radius, and laminar flow with no change in radial velocity. The methodology involved subdividing the water circuit into mostly equal volume elements ($\sim 5 \text{ cm}^3$) and transporting water along the pipe in discrete time steps. A couple of elements on the bend of the mock-up were difficult to split, however, this slight variation had a negligible effect in comparison with the uncertainty on the measured volume of the mock-up, at 0.6%. The $^{16}\text{O}(n, p)^{16}\text{N}$ reactions rates were calculated in FISPACT-II [11] using EAF-2010 [12], TENDL-2014 [13], ENDF/B-VII.0 [14], and JEFF-3.2 [15], and in MCNP using ENDF/B-VII.1 [16], FENDL-3.1d, FENDL-2.1 [17], FENDL-3.0 [10], ENDF/B-VII.0, and JEFF-3.3 [18]. However, in MCNP the N-16 cross-sections in each library originate from ENDF/B-VII.1 generating identical reaction rates, therefore only one MCNP library has been considered to present reaction rates in this paper. This information was fed into the GammaFlow code, when the water element is within a defined neutron irradiation region N-16 atoms the reaction rates were used to add inventory for that pipe element. The code also tracks the decay of N-16 atoms as the water moves through the circuit. In MCNP all calculations were run for 1×10^7 histories to enable results with statistical error in the reaction rates to be less than 1% for each cell, with all cells passing the statistical tests in MCNP indicating convergence. The reaction rates per source neutron calculated for N-16 in each element of the mock-up component, with the mock-up positioned at 5 cm and 2 cm, are displayed in Figures 4 and 5, respectively.

Figures 4 and 5 show the peak reaction rate in element #18 which is 2.03×10^{-6} N-16 atoms per source neutron per cm^3 and 6.18×10^{-6} N-16 atoms per source neutron per cm^3 , for the 5 cm and 2 cm cases respectively.

3.1. CsI detector modelling

A large CsI scintillator ($\sim 25 \text{ cm}$ diameter and $\sim 20 \text{ cm}$ height) coupled to a photo-multiplier tube was used to measure the gammas from N-16. The CsI detector was placed behind a 1 m thick concrete shield wall $\sim 15 \text{ m}$ from the FNG source to shield from neutrons,

and was surrounded by a 5 cm thick copper layer and 10 cm of lead to reduce background noise. A detailed MCNP model of the CsI detector was provided by ENEA, and included the CsI tank containing a wedge-shaped deflector (to enable water mixing within the expansion tank) that was placed 13.5 cm from the CsI detector end-cap, as shown in Figure 6.

The measured energy resolution of the CsI was incorporated in MCNP using the Gaussian Energy Broadening (GEB) function, where $a = 0.00348739$, $b = 0.068802$, and $c = 0.0992018$. The CsI efficiency between 5.5-6.5 MeV (corrected for the branching ratio) was calculated to be 2.32%, based on a gamma source term including the inlet and outlet pipes as well as the water inside the expansion tank. The source definition assumed in MCNP to determine the efficiency used emission probabilities based on volume averaged activities for each of the regions.

4. Results

The measured results and results calculated using GammaFlow and EASY-2007 are presented in Table 1. The calculated CPS values were obtained by multiplying the activity at the CsI detector, output from GammaFlow, with the CsI efficiency and branching ratio. The measured CPS values were obtained from the count rate in the 5.5-6.5 MeV energy region, after background subtraction. The C/E values compare measured results with results calculated using GammaFlow (CCFE C/E) and with results calculated by ENEA (ENEA C/E). The method employed by ENEA used the EASY-2007 code system [19], an early FISPACT-II code which uses the EAF-2007 nuclear data library. In EASY-2007 the input parameters included the flux of the FW mock-up, for each measurement scenario, the mass of water (assuming no impurities), and the decay time determined from the TOF. The uncertainties in the C/E values have been summed in quadrature and consider a 10% contribution for the $^{16}\text{O}(n, p)^{16}\text{N}$ reaction from the EAF-2010 nuclear data library [12], 5% uncertainty in the efficiency of the CsI detector from the calibration and detector modelling [20], 4% for the evaluation of the FW mock-up neutron flux due only to FNG yield uncertainty since Monte Carlo statistical errors are negligible, 0.9-5% uncertainty on the TOF (the higher the water speed the higher the uncertainty), 0.6% uncertainty from the FW mock-up volume. Note that it was not possible to include uncertainties from any other nuclear data libraries due to formatting issues for the ENDF/B libraries (most others are based on these for ^{16}O); a potential alternative method to assess the sensitivity of results to the nuclear data could use a total Monte Carlo (TMC) approach, for example using TENDL perturbed files, but this is beyond the scope of the present work.

The results are illustrated in Figs. 7–10. The top section of each figure provides a comparison between the nuclear data libraries used for the GammaFlow calculations. The middle sections provides a comparison between the EAF-2010 library used for the GammaFlow calculations, and the results calculated by ENEA. While the bottom sections compares the averaged CCFE C/E values with the ENEA C/E values. For circuit #2, at low flow rates (10-15 Hz) the calculated values are clearly underestimating the measured count rate. This is thought to result from a lack of complete mixing assumed by the simulations within the JCC-15 expansion tank, which means water is passing more directly to the CsI expansion tank leading to a higher count rate.

5. Discussion and conclusions

A water activation experiment was performed at the FNG to validate the simulation for water activation assessment used for ITER and to provide scientific justification to reduce safety factors. This paper has provided a comparison of measured activities of N-16 with results calculated using GammaFlow and using EASY-2007. Reaction rate data was extracted for five nuclear data libraries using MCNP6.1 with

Table 1

C/E values with uncertainties calculated for different flow rates, for circuit #1 and #2 with the mock-up positioned at 5 cm and 2 cm. A TOF comparison between experimental values and values calculated using GammaFlow is also presented.

	Pump frequency (Hz)	Flow rate (litre/min)	TOF through mock-up (s)	TOF to CsI detector (s)		Calculated CPS	Measured CPS	CCFE		ENEA		
				Measured	Calculated			C/E	Error ±	C/E	Error ±	
Circuit #1	5 cm	10	10.3	1.894	10.7	10.8	1824	1993	0.92	0.11	0.97	0.12
		15	16.4	1.186	6.7	6.8	1714	1922	0.89	0.11	0.96	0.12
		20	22.0	0.885	5.0	5.1	1519	1697	0.90	0.11	0.97	0.12
		25	27.5	0.708	4.0	4.0	1345	1507	0.89	0.11	0.97	0.12
		30	34.4	0.566	3.2	3.2	1166	1344	0.87	0.11	0.95	0.12
	35	39.4	0.496	2.8	2.8	1062	1228	0.86	0.11	0.95	0.12	
	40	44.1	0.443	2.5	2.5	978	1125	0.87	0.11	0.96	0.13	
	45	50.1	0.389	2.2	2.2	887	1031	0.86	0.11	0.95	0.13	
	50	55.1	0.354	2.0	2.0	823	948	0.87	0.11	0.96	0.13	
	2 cm	10	10.1	1.912	10.8	10.9	3298	3361	0.98	0.12	1.05	0.13
		15	16.0	1.204	6.8	6.9	3119	2982	1.05	0.13	1.14	0.13
		20	21.8	0.885	5.0	5.1	2756	2684	1.03	0.12	1.12	0.13
		25	27.3	0.708	4.0	4.0	2441	2382	1.02	0.12	1.13	0.13
		30	34.1	0.566	3.2	3.2	2117	2121	1.00	0.12	1.10	0.13
	Circuit #2	5 cm	10	13.3	1.448	15	15.1	434	852	0.51	0.11	0.56
15			19.2	1.004	10.4	10.5	686	1025	0.67	0.10	0.74	0.12
20			25.0	0.772	8.0	8.0	772	1008	0.77	0.11	0.84	0.12
25			29.4	0.656	6.8	6.8	780	924	0.85	0.11	0.93	0.12
30			37.1	0.521	5.4	5.4	755	916	0.83	0.11	0.91	0.12
35		41.7	0.463	4.8	4.8	718	885	0.81	0.11	0.89	0.12	
2 cm		10	13.9	1.390	14.4	14.5	782	1407	0.55	0.13	0.62	0.12
		15	19.6	0.984	10.2	10.3	1238	1732	0.71	0.12	0.79	0.12
		20	25.7	0.753	7.8	7.8	1395	1741	0.80	0.11	0.89	0.12
		25	30.3	0.637	6.6	6.6	1409	1722	0.81	0.11	0.91	0.12
		30	37.1	0.521	5.4	5.4	1365	1669	0.81	0.11	0.91	0.12
35		43.5	0.444	4.6	4.6	1298	1590	0.81	0.11	0.90	0.12	

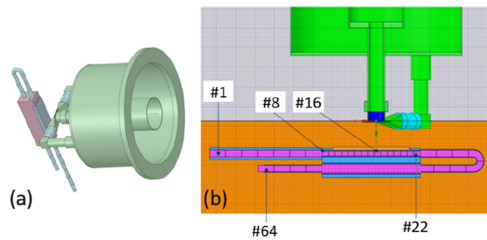


Fig. 3. (a) shows a 3D model of the FNG (in green) and the FW mock-up (in purple and blue), (b) a CAD image showing the sub-division of the water regions inside the mock-up with some of the water element numbers indicated.

pointwise libraries and FISPACT-II with group-wise libraries and fed into GammaFlow to calculate the N-16 activity at the CsI detector position assuming laminar water flow rate. Good agreement was found between the nuclear data libraries ENDF/B-VII.1, EAF-2010, TENDL-2014, ENDF/B-VII.0 and JEFF-3.2 for the $^{16}\text{O}(n, p)^{16}\text{N}$ reaction, with a factor of 1.12 and 1.11 in reaction rate between the highest and lowest values for element #18, with the mock-up at 5 cm and 2 cm respectively.

The results calculated by ENEA used the TOF between the outlet of the FW mock-up and the outlet of the CsI expansion tank as the decay time, the activity of the water was then averaged across the volume of the CsI tank and combined with the CsI efficiency and branching ratio

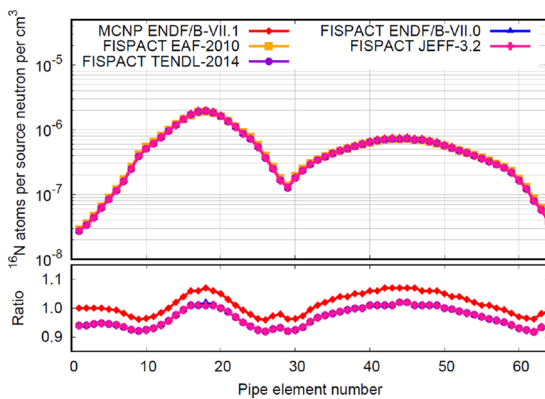


Fig. 4. Reaction rates per element for N-16 derived inside the mock-up component, at 5 cm from the FNG source, using MCNP6.1 and FISPACT-II.

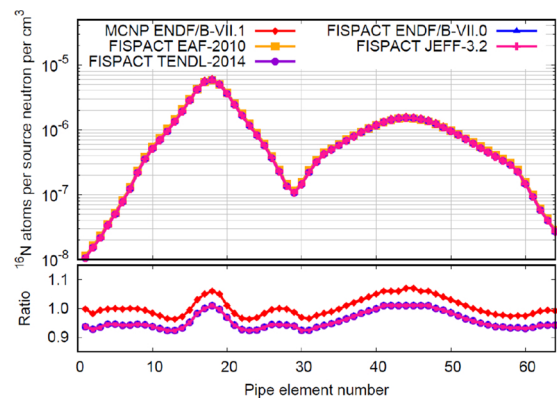


Fig. 5. Reaction rates per element for N-16 derived inside the mock-up component, at 2 cm from the FNG source, using MCNP6.1 and FISPACT-II.

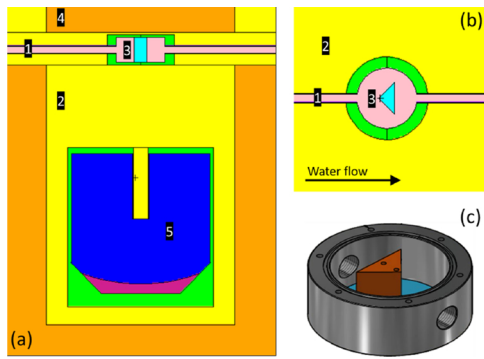


Fig. 6. MCNP model showing (a) the XY plane at Z=0 cm slice of the CsI detector and CsI expansion tank and (b) the XZ plane at Y=14 cm slice of the CsI expansion tank (c) CsI expansion tank taken from the CAD drawing. In (a) and (b) label 1 indicates the water pipes, 2 indicates regions of air, 3 shows the CsI water expansion tank with an aluminium wall in green and deflector wedge in turquoise, 4 indicates the copper shield in orange (lead not shown), and 5 shows the CsI detector crystal in blue (with the dead-layer in purple). The direction of water flow is indicated in (b).

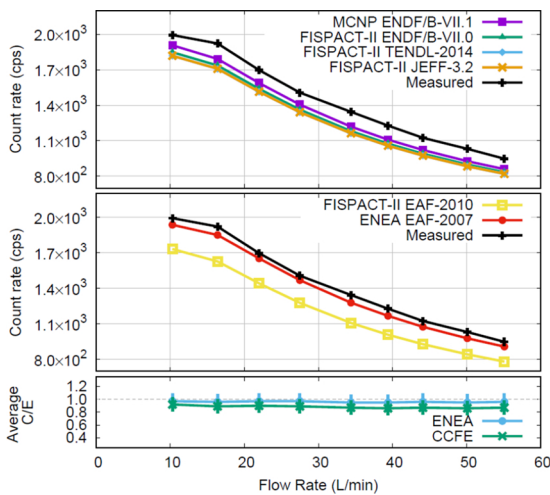


Fig. 7. The count rate calculated for N-16 in the CsI detector with the mock-up at 5 cm in the 5.5-6.5 MeV range for circuit #1 at various water flow rates.

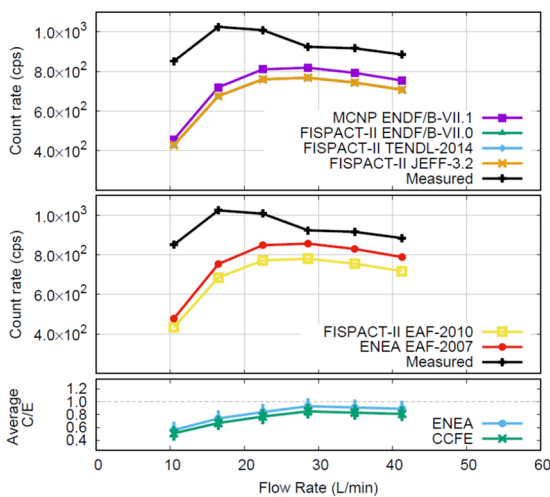


Fig. 8. The count rate calculated for N-16 in the CsI detector with the mock-up at 5 cm in the 5.5-6.5 MeV range for circuit #2 at various water flow rates.

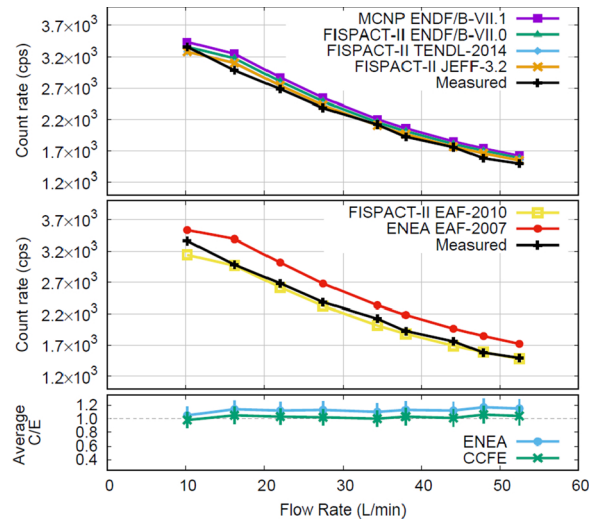


Fig. 9. The count rate calculated for N-16 in the CsI detector with the mock-up at 2 cm in the 5.5-6.5 MeV range for circuit #1 at various water flow rates.

to provide the calculated CPS results. Whereas GammaFlow modelled the movement of water through the circuit and calculated the activity of the water at the inlet and outlet of the CsI tank, the averaged result was combined with the detector efficiency and branching ratio to provide the calculated CPS results. This slight difference in the methodology resulted in systematic differences in the C/E results presented in Figures 7 - 10. A benefit of GammaFlow is the potential to account for physical effects such as water mixing, pipes splitting and recombining, non-homogeneous activity distributions. The version of GammaFlow used in this work does not take these effects into account, however, future versions of the code currently under development will look to incorporate these effects to provide improved simulation capabilities.

The data provided in Table 1 shows a comparison in the calculated and measured TOF between the FW mock-up and CsI tank, with an average percentage difference of 0.77% showing excellent agreement with measured TOF values and suggesting the water circuit was well-defined in GammaFlow. The overall CCFE C/E value, an average over the four measurement scenarios, was 0.87 ± 0.11 , which shows good agreement with the simulated results using GammaFlow. The average ENEA C/E value was 0.95 ± 0.12 , showing agreement to within 1σ of

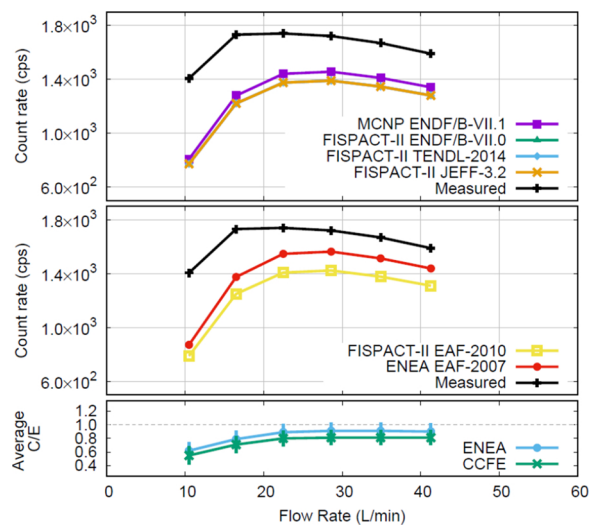


Fig. 10. The count rate calculated for N-16 in the CsI detector with the mock-up at 2 cm in the 5.5-6.5 MeV range for circuit #2 at various water flow rates.

the average CCFE C/E, hence validating the methodology presented in this paper for simulating water activation assessments.

Declaration of interests

None.

Acknowledgements

The UKAEA were subcontracted by ENEA to complete this work which was funded by Fusion for Energy under the Contract F4E-OPE-0956. This publication reflects the views of the authors only, and Fusion for Energy cannot be held responsible for any use which may be made of the information contained therein. The views and opinions expressed herein do not necessarily reflect those of the ITER Organization.

References

- [1] (data sourced from the Evaluated Nuclear Structure Data Files (ENSDF) snapshot March 2018, IAEA website accessed: 04/03/2019). <https://www-nds.iaea.org>.
- [2] S. Jakhar, et al., Calculation of activation water radiation maps in ITER, *Neutronics Challenges of Fusion Facilities-II, Transactions of the American Nuclear Society* 116 (2017).
- [3] Nuclear Analysis of 16N and 17N radiation fields from TCWS activated water, IDM Number: ITER_D_QZ7BEK_v2.1, 16/11/2016.
- [4] M. Angelone, et al., Measurements of delayed neutron emission from water activated by 14 MeV neutrons in a FW mock-up of ITER, preprint submitted to ISFNT, 2019.
- [5] C.R. Nobs, GammaFlow Code Development at UKAEA (memo), TechD-20-093 (2019).
- [6] M. Pillon, et al., Comparison between measurement and calculations for a 14 MeV neutron water activation experiment, preprint submitted to ND2019, 2019.
- [7] M. Martone, M. Angelone, M. Pillon, *The 14 MeV Frascati Neutron Generator, Journal of Nuclear Materials* 212 (1994) 1661–1664.
- [8] MCNP6 Development Team, Initial MCNP6 Release Overview MCNP6 Version 1.0, Los Alamos National Laboratory report LA-UR-13-22934.
- [9] R.J. McConn Jr. et al., *Compendium of Material Composition Data for Radiation Transport Modeling, Revision 1* (2011).
- [10] R.A. Forrest, et al., FENDL-3 library - Summary document INDC(NDS)-628 (2012); FENDL-3.1d is available at <https://www-nds.iaea.org/fendl/index.html>.
- [11] J.C. Sublet, et al., FISPACT-II: An Advanced Simulation System for Activation, *Transmutation and Material Modelling* 139 (2017) 77–137.
- [12] J.Ch. Sublet, et al., The European Activation File: EAF-2010 neutron induced cross section library, CCFE-R(10) 05, 2010.
- [13] M. Fleming, et al., Probing experimental systematic trends of the neutron-induced TENDL-2014 nuclear data library, CCFE report UKAEA-R(15)29, 2015.
- [14] M.B. Chadwick, et al., ENDF/B-VII.0: Next generation evaluated nuclear data library for nuclear science and technology, *Nuclear Data Sheets* 107 (12) (2006) 2931–3060.
- [15] The JEFF team, JEFF-3.2: Evaluated nuclear data library. <http://www.oecdnea.org/dbdata/jeff/>. Release date: March 2014.
- [16] M.B. Chadwick, et al., ENDF/B-VII.1 nuclear data for science and technology: Cross sections, covariances, fission product yields and decay data, *Nuclear Data Sheets* 112 (12) (2011) 2887–2996.
- [17] D.L. Aldama, A. Trkov, FENDL-2.1: Update of an evaluated nuclear data library for fusion applications, IAEA Report INDC(NDS)-467 (2004).
- [18] JEFF team, JEFF-3.3: Evaluated nuclear data library. <https://www.oecd-nea.org/dbdata/jeff/jeff33/index.html>. Release date: November 2017.
- [19] R.A. Forrest, et al., EASY-2007: a new generation of activation modelling including neutron-, proton- and deuteron-induced reactions, 196, 2008.
- [20] M. Pillon, Private communication, 04/10/2017.